KfK 2586
August 1978

Summary of Results for the SNEAK-9 Series of Critical Experiments and Conclusions for the Accuracy of Predicted Physics Parameters of the SNR-300

compiled by: F. Helm
Institut für Neutronenphysik und Reaktortechnik
Projekt Schneller Brüter

Kernforschungszentrum Karlsruhe

KERNFORSCHUNGSZENTRUM KARLSRUHE
Institut für Neutronenphysik und Reaktortechnik
Projekt Schneller Brüter

KfK 2586

Summary of Results for the SNEAK-9 Series of Critical Experiments and Conclusions for the Accuracy of Predicted Physics Parameters of the SNR-300

compiled by

F. Helm

with contributions from

R. Böhme, G. Durance [1], P. Fehsenfeld, E.A. Fischer, S. Ganesan [2], H. Giese, G. Henneges, G. Jourdan, R. Kiesel, P. McGrath, U. v. Möllendorff, W.J. Osterkamp, S. Pilate [3], M. Pinter, A.M.Elbel-Raberain, W. Scholtyssek, G. Wittek

1) Delegatefrom AAEC, Sydney, Australia
2) Delegatefrom Reactor Research Centre Kalpakkam, India
3) Belgonucleaire, Brussels

Kernforschungszentrum Karlsruhe GmbH., Karlsruhe

Summary of Results for the SNEAK-9 Series of Critical Experiments and Conclusions for the Accuracy of Predicted Physics Parameters of the SNR-300

Abstract

In a series of critical assemblies in SNEAK physics parameters of interest for the prototype fast reactor SNR-300 were investigated and compared to the results of calculations. Since a complete mock-up of the SNR-300 was not possible with the material supply available the measurements were performed in three different assemblies, each being adapted to the investigation of a particular set of problems.

Work was concentrated on the following quantities: criticality, breeding ratio, Na-void effect, control rod worths and power distribution.

The calculations were performed using the diffusion and transport methods available at KFK and as a data basis the KFKINR cross section set.

Detailed descriptions of the assemblies, the majority of the results and extensive discussions of the experimental and calculational methods used can be found in separate KFK reports about each assembly which were already published.

This report contains a summary of the results for each quantity investigated including a basic account of the methods used, and an evaluation of the significance of these data for the prediction of parameters of the SNR-300.

Zusammenfassung der Ergebnisse für die Reihe SNEAK-9 kritischer Anordnungen und Folgerungen für die Vorhersagegenauigkeit von physikalischen Eigenschaften des SNR-300

Zusammenfassung

In einer Reihe kritischer Anordnungen in SNEAK wurden physikalische Eigenschaften, die für den schnellen Prototyp Reaktor SNR-300 von Interesse sind, untersucht und mit den Ergebnissen von Berechnungen verglichen. Da ein vollständiger Nachbau des SNR-300 mit den verfügbaren Materialien nicht möglich war, wurden die Messungen in drei verschiedenen Anordnungen durchgeführt, von denen jede im Hinblick auf die Untersuchung bestimmter Problemstellungen entworfen worden war.

Die wichtigsten Größen, auf die sich die Untersuchungen konzentrierten, waren: Kritikalität, Brutrate, Na-void Effekt, Kontrollstabwerte und Leistungsverteilung.

Die Berechnungen wurden mit den im KFK verfügbaren Diffusions- und Transportmethoden durchgeführt. Die Datenbasis war der KFKINR-Wirkungsquerschnittssatz.

Eingehende Beschreibungen der Anordnungen, der größte Teil der Ergebnisse und eine genaue Beschreibung der Meß- und Rechenmethoden wurden bereits in eigenen KFK-Berichten für jede Anordnung veröffentlicht.

Der vorliegende Bericht enthält eine Zusammenfassung der Ergebnisse für jede der untersuchten Größen, die wichtigsten Angaben über die angewandten Methoden und eine Bewertung der Daten im Hinblick auf die Vorhersage von physikalischen Eigenschaften des SNR-300.

Table of Contents

1. Introduction

The series of critical experiments SNEAK-9 was conceived to provide the main experimental basis for the prediction of physics parameters of the fast breeder prototype SNR-300. Since the materials available at SNEAK did not allow the construction of a full core mock-up, a number of assemblies was built representing the most important neutronic characteristics of the prototype. Each assembly was designed in such a way that the accuracy of calculations for specific parameters could be tested and that the deviations found between measurements and calculations could be used to improve the predictions for the power reactor. The assemblies were investigated in the following sequence:

SNEAK-9B (1972), an assembly simulating the composition of the SNR-300 in a central zone of 43.4 cm radius and in the corresponding part of the axial blanket /1/. The test zone contained SNEAK PuO_2UO_2 fuel, Na, and depleted uranium and was surrounded radially by a driver fueled with enriched uranium (Fig. 1). This core was mainly suitable for measurements of the Na-void effect (axially along the core axis and for large central voids) and for measurements of reaction rates for the determination of the breeding gain (^{239}Pu fiss and ^{238}U capt) along the core axis and through the axial blanket; also central absorber worth measurements and Doppler measurements with heated samples were performed.

SNEAK-9A (1973/74), a two-zoned uranium fueled core which gave a quite close simulation of the geometrical properties and the control rod arrangement of the SNR-300 /2,3/. This assembly was investigated in three modifications: 9A-0 with no simulated control rods in its basic configuration; 9A-1 with all control rods simulated in the withdrawn position, and 9A-2 with all regulating rods simulated with the absorber

Zum Druck eingereicht am 29.8.78

half inserted and all safety rods simulated withdrawn (Fig. 2). The main objective of SNEAK-9A was to measure control rod worths, particularly for bank insertion, and power distributions for a number of rod insertion patterns.

SNEAK-9C (1974/75), a single zone assembly /4/ which, in its most important modification, SNEAK-9C-2, used a core cell of one PuO_2UO_2 platelet and one Na platelet (Fig. 3). SNEAK-9C-1 was a preceding uranium fueled assembly of about equal size which was transferred into 9C-2 by a sector substitution in order to test if criticality changes caused by introduction of a sector of different composition could be extrapolated to a substitution of the whole core. SNEAK-9C-2 was the only core built for investigating the parameters of the SNR-300 which was fueled entirely with plutonium. In order to achieve criticality with the SNEAK plutonium supply the core had to be rather small (247 ℓ) and highly concentrated in fuel. Besides being the final step of the sector substitution it served to check criticality prediction for an all plutonium core and as a test bed for a series of Na-void experiments. In the modifications 9C-2/POS and 9C-2/POZ test zones were introduced containing plutonium with a higher ^{240}Pu contents, mainly to measure the influence of the higher Pu-isotopes on criticality and Na-void effect. The same parameters were investigated in 9C-2/C for a carbide test zone with high ^{240}Pu contents. Measurements of reaction rates for the determination of the breeding gain were also performed in SNEAK-9C-2.

All calculations were performed with the KFKINR set of cross sections /5/. More information on the calculational methods will be given in the sections on the individual parameters. This report will give a survey of all the experimental and calculated results and of the conclusions which can be drawn for the prediction of the physics parameters of the SNR-300.

2. k_{eff} and Critical Mass

2.1 Clean critical size

For each of the assemblies reported here a configuration called the "clean critical" was established. For this purpose the minimum number of fuel elements for which the assembly could just be made critical was determined and arranged in the most symmetric way possible. Then exact criticality was established by adjusting one of the SNEAK control rods. This control rod was calibrated by the inverse kinetics technique, so the exact k_{eff} of the clean critical configuration could be determined.

2.2 Methods of k_{eff}-calculation

The basic calculation for each assembly was a two-dimensional RZ diffusion calculation in 26 energy groups, performed with the program DIXY /6/. In this calculation parts of the assembly which cannot be approximated by the cylindrical geometry (e.g. simulated control rods) had to be smeared into rings. For calculating the cross sections of each region, a homogeneous mixture of the materials was assumed.

A cylinderisation correction was derived from a comparison of an XY calculation in which the geometry of the assembly in the horizontal plane was represented as closely as possible, and a one-dimensional cylinder calculation using the same radial geometry as the RZ calculation. In both cases vertical bucklings determined from the axial flux distribution in the RZ calculation were used.

For the determination of the heterogeneity correction effective cross sections for the plate cells were calculated by integral transport theory /7/ (collision probability method). The effect of the transition from homogeneous cross sections to cell averaged cross sections taking into account the heterogeneity was then calculated in one dimension and simplified geometry.

A general transport correction was found by comparing transport and diffusion calculations. These were performed either one-dimensional (axial and radial) or two-dimensional (in RZ geometry).

Special transport corrections had to be derived for the effects of simulated SNR-300 control rods. Since for this purpose the axial and the radial dimension of the rod must be represented properly the calculations were performed in RZ geometry for the central position. The effect for excentrical rods was derived by multiplying with the ratio of material worths at the central position and at the actual rod position.

Further corrections considered were:

The REMO correction. It represents an improvement of the group averaging of the elastic downscattering cross section /8/.

The CHI correction. It accounts for the difference in the fission spectra in the different reactor zones. The basic calculations always used one spectrum for all regions.

The effect of the last two corrections is of the order of 0.1 % only. It was not calculated for all assemblies.

For the SNEAK-9A assemblies also three-dimensional synthesis calculations in 4 energy groups with the code KASY /9/ were performed. Their result should correspond to that of the basic RZ calculation plus the cylinderization correction. The maximum deviation found from this value was -0.16 % in SNEAK-9A-1.

2.3 Results from the basic assemblies

Table 1 shows the results of the calculations including all corrections for the basic assemblies of the series. The final result of all assemblies lies in the range C/E = 1.008 ± 0.0025.

This positive deviation of the calculated k_{eff} is probably mostly due to an underestimate of leakage, only partially compensated by an overestimate of $^{238}U_{capt}$. This (qualitative) analysis is supported by the following arguments:

- In the cores SNEAK-7A and 7B /10/, where the leakage was measured via central worth measurements of core material it was calculated 6 % and 10 % low, respectively.
- The KFKINR set calculates $^{238}U_{capt}$ on the average about 4 % high.
- The k_{eff} of small assemblies (SNEAK-9C, 7A, 7B) tends to be calculated high, while the k_{eff} of assemblies with low leakage is calculated lower (SNEAK-10 /11/: ∿ 1.002, k_∞-zone of SNEAK-8 /12/: 0.91).

The composition of the SNEAK-9 cores is essentially representative for the SNR-300. (The results in Table 1 show, that the use of uranium or plutonium fuel does not cause much difference). The leakage fraction of the SNR-300 lies between that of SNEAK-9A and 9B on the one hand and SNEAK-10 on the other. Without consideration of differences caused by heterogeneity, Pu-isotopic vector and burn-up one would therefore expect a C/E ratio of 1.006 ± 0.003 for the k_{eff} of the SNR-300.

2.4 Consequences of the substitution experiments

In SNEAK-2 the critical size of a fully plutonium-fueled core of the geometry of the SNR-300 was extrapolated using a 90^{o} sector substitution from the uranium fueled core SNEAK-2A to the plutonium sector core SNEAK-2B /13/. The validity of such a procedure was checked by the sector substitution SNEAK-9C-1 to SNEAK-9C-2 which was carried through to the full plutonium core /14/. The result of this test was that a 90^{o} substitution can actually be extrapolated to a fully substituted core with an uncertainty of about 0.003 in k_{eff}.

Now, Pilate /15/ calculated the full plutonium core extrapolated from the SNEAK-2B substitution with the KFKINR cross section set using the methods described above (section 2.2). His results are the following:

Calc./Exp. for k_{eff} of SNEAK-2B (extrapolated):

2 dim. (RZ) DIXY 26 gr.	1.0045
Δk cyl.	-0.0012
Δk het.	-0.0005
Δk trans.	+0.0093
REMO	+0.0008
CHI	+0.0018
k_{eff} (corr.)	1.0147

The final result is about 0.007 higher than the average criticality prediction of the SNEAK-9 assemblies and considerably outside the variance found for these and other SNEAK assemblies. A closer examination shows that the basic diffusion calculation and the CHI-correction each lie about 0.002 above what might be expected from comparisons with other assemblies - the other corrections lie about in the expected range. A definite reason for the deviation cannot be given as of now.

Table 1 Criticality Predictions for SNEAK-9 Cores

Assembly	9B	9A-0	9A-1	9A-2	9C-1	9C-2
2 dim. (RZ) DIXY / 26 gr.	1.0026	0.9959	0.9977	0.9944	1.0041	1.0014
Δk_{cyl}	-0.0021	-0.0014	-0.0067	-0.0020	-0.0020	-0.0040
Δk_{het}	-0.0006	+0.0060	+0.0055	+0.0050	+0.0005	-0.0010
Δk_{trans}	+0.0059	+0.0062	+0.0058	+0.0058	+0.0093	+0.0124
$\Delta k_{tr\ rod}$			+0.0060	+0.0044		
REMO	+0.0007				-0.0016	+0.0002
CHI					+0.0002	-0.0010
k_{eff} (corr.)	1.0065	1.0067	1.0083	1.0076	1.0105	1.0080

For the purpose of criticality prediction of the SNR-300 it appears advisable to retain the conclusions of section 2.3 as they are supported by numerous SNEAK cores and in addition by evaluations of ZPPR 2 and ZPPR 4, also performed by Pilate /16/, which yield C/E-values for k_{eff} (corr.) in the range between 1.0045 and 1.009.

Nevertheless a full explanation of the sector substitution results would be very desirable for increased confidence in the predictions derived from SNEAK-9 and other assemblies.

2.5 The influence of the plutonium isotopic vector

The transfer of the results of criticality determination in SNEAK-9 to the power reactor SNR-300 is complicated by the difference in the isotopic vector of the plutonium. In order to improve this situation the following quantities of plutonium with increased higher isotopes contents were made available for experiments in SNEAK-9C-2:

32.98 kg PuO_2UO_2 purchased from ENEL and VAK
85 kg Pu-metal borrowed from the UKAEA

The isotopic contents of the SNR-300 fuel (as stated at different stages of planning) and of the platelets used in the SNEAK-9 experiments compare as follows:

Table 2 Isotopic Vectors of Various Fuels

Type of fuel	Weight percent			
	^{239}Pu	^{240}Pu	^{241}Pu	^{242}Pu
SNR-300 original plan	75	22	2.5	0.5
SNR-300, new plan				
inner zone	75.25	20.25	3.75	0.75
outer zone	60	24	13	3
SNEAK, PuO_2UO_2 normal plates	91.26	8.24	0.47	0.03
SNEAK, PuO_2UO_2 ENEL/VAK	72.19	19.33	6.39	1.62
UKAEA Pu-metal plates	77.68	18.91	2.79	0.62

Zones of increasing size using ENEL/VAK plates in the one case and UKAEA metal plates in the other were introduced into the center of SNEAK-9C-2. Besides this, the material worth was measured for ^{240}Pu and ^{241}Pu samples in the center of several assemblies.

The zones with the ENEL/VAK-PU had the shape of a cube with the side-length increasing from about 10 cm to 32 cm. For the UKAEA-metal substitution the test zones extended axially through the whole core, the effective radius of the zone was increased from 6.14 cm (4 elements) to 21.7 cm (50 elements). In both cases it was found that the reactivitiy effect was quite closely proportional to the statistical weight of the substituted zone, allowing an easy extrapolation to the fully substituted core.

Measured and extrapolated changes of k_{eff} and C/E values for the actually measured and the extrapolated cases are given in Table 3.

Table 3 Results for the Substitution of Zones with an Increased Contents of higher Pu-Isotopes

Assembly loading	Δk against basic assembly (measured or extrapolated from measurement)	C/E for k_{eff}
basic SNEAK-9C-2	-	1.0080 ± 0.001
PuO_2UO_2 ENEL/VAK largest substituted zone	-0.00199	1.0076 ± 0.001
PuO_2UO_2 ENEL/VAK extrapolated to whole core	-0.00663	1.0067 ± 0.0015
Pu-metal UKAEA largest substituted zone	+0.00110	1.0050 ± 0.001
Pu-metal UKAEA extrapolated to whole core	+0.00207	1.0023 ± 0.0015

The final error cited is mainly caused by uncertainties in plate data. The largest change in C/E for k_{eff} is found for the case of the use of UKAEA metal plates. This may be due to an insufficiently accurate calculation of the heterogeneity effect for this type of plates which amounts to about 1 % while it is only around -0.1 % for the SNEAK mixed oxide plates. So the only conclusion which can be drawn from these experiments is that the effect of the changed isotopic vector on the deviation of k_{eff}-calculations does not exceed greatly the value of 0.5 %.

For the material worth measurements of ^{240}Pu and ^{241}Pu the following results were found in the cores of SNEAK-9:

Table 4 Results of Material Worth Measurements with ^{240}Pu and ^{241}Pu

Assembly	9B	9A	9C-2
$\rho(^{240}Pu)/\rho(^{239}Pu)$	0.200	0.135	0.201
C/E for this number	0.93	1.09	1.23
$\rho(^{241}Pu)/\rho(^{239}Pu)$	1.52	1.35	1.19
C/E for this number	0.89	1.04	1.06

It appears that there is still a large scatter and no well established bias in these data. When going from the normal SNEAK fuel to the SNR-300 fuel the change of concentration of these isotopes corresponds to about 2 % in k_{eff} for each. Since the C/E values for their material worth scatter by 17 to 30 % one arrives at a uncertainty of about 0.5 % in the k_{eff} of the SNR-300 due to the presence of higher Pu-isotopes. This is essentially in agreement with the result of the central zone measurements.

2.6 Improvement of the prediction of the burn-up reactivity

The main contributions to the burn-up reactivity of the SNR-300 arise from the consumption and production of the isotopes ^{239}Pu and ^{241}Pu and from fission products. In SNEAK-9, measurements suited to reduce the uncertainty of burn-up reactivity were the determination of delayed neutron parameters and measurements of reactivity worths and reaction rates for ^{239}Pu and ^{241}Pu:

Measurements of β_{eff} and of ratios of β for various isotopes enabled Fischer /17/ to confirm delayed neutron data proposed by Tuttle /18/ (see also section 7). This gave a new basis for the evaluation of material worths and when applied to ^{239}Pu essentially eliminated the central worth discrepancy for this material. This also was confirmed by material worth measurements in SNEAK-9 cores:

Table 5 C/E ratios for the material worth of ^{239}Pu in the assemblies

β_{eff}-Data from	9B	9A	9C-1	9C-2
Keepin /26/	1.10	1.10	1.06	1.05
Tuttle /18/	1.02	1.02	1.02	0.99

The improvement shown means a reduction of the uncertainty of the worth of ^{239}Pu to about 5 %.

The measured and calculated material worths of ^{241}Pu as shown in Table 4, section 2.5 indicate an uncertainty of 17 % for this isotope.

Fission rate measurements for ^{241}Pu were performed for the first time in SNEAK in the assemblies 9C-2 and 9C-2/POS. For this purpose miniature fission chambers for insertion into the unit cell with minimum perturbation had to be manufactured. The agreement of the measurements with calculations was very good. For the ratio $\sigma_f{}^{241}Pu/\sigma_f{}^{235}U$ the results were

	9C-2	9C-2/POS
$C/E\left(\frac{\sigma_f{}^{241}Pu}{\sigma_f{}^{235}U}\right)$	1.001	0.990

The estimated uncertainty in the ^{241}Pu fission rate thereupon was reduced from 20 % to 12 %, and it can be reduced further if the good agreement can be confirmed in further measurements.
For the capture rate of ^{241}Pu an experimental worth derived from fission rate and material worth was found which agreed within 2 % with the calculated value. Therefore the uncertainty in this parameter also could be reduced.

Table 6 Contribution to the Uncertainty in the Prediction of the Burn-up Reactivity [a) b)]

Parameter	Uncertainty of parameter old	Uncertainty of parameter new	Weight [c)] Normal Pu [d)]	Weight [c)] LWR Pu [d)]	Uncertainty of burn-up reactivity: Normal Pu old	Uncertainty of burn-up reactivity: Normal Pu new	Uncertainty of burn-up reactivity: LWR-Pu old	Uncertainty of burn-up reactivity: LWR-Pu new
$\rho(^{239}Pu)$	<u>0.1</u>	<u>0.05</u>	0.83	0.72	<u>0.083</u>	<u>0.041</u>	<u>0.072</u>	<u>0.036</u>
$\rho(^{241}Pu)$	<u>0.25</u>	<u>0.17</u>	0.06	0.34	<u>0.015</u>	<u>0.010</u>	<u>0.085</u>	<u>0.058</u>
ρ(Fiss.Prod.)	0.2	0.2	0.25	0.22	0.050	0.050	0.044	0.044
$R_f(^{239}Pu)$	0.01	0.01	0.57	0.35	0.006	0.006	0.004	0.004
$R_c(^{239}Pu)$	0.2	0.2	0.33	0.25	0.066	0.066	0.050	0.050
$R_c(^{238}U)$	0.04	0.04	0.8	0.62	0.032	0.032	0.025	0.025
$R_f(^{241}Pu)$	<u>0.2</u>	<u>0.12</u>	0.08	0.16	<u>0.016</u>	<u>0.010</u>	0.032	<u>0.019</u>
$R_c(^{241}Pu)$	<u>0.4</u>	<u>0.24</u>	0.03	0.07	<u>0.012</u>	<u>0.007</u>	<u>0.028</u>	<u>0.017</u>
$R_c(^{240}Pu)$	0.3	0.3	0.103	0.08	0.031	0.031	0.024	0.024
others					0.055	0.055	0.055	0.055
Total uncertainty					0.139	0.118	0.151	0.118

a) All data refer to 1.7 $\sigma \sim$ 90 % confidence level

b) Values were improvements have taken place are underscored

c) Weight: <u>induced uncertainty in burn-up reactivity</u> / uncertainty of a parameter

d) Isotopic vectors

Normal Pu 73.5/22/3.75/0.75

LWR Pu 65/22/10/9

Table 6 shows for plutonium of two different isotopic vectors the most important uncertainties in material worth and reaction rates before and after the evaluation of the SNEAK-9 experiments. Also given is for each parameter its weight in the burn-up determination and its influence on the uncertainty of the burn-up. It is interesting to see the increased importance of ^{241}Pu when LWR-plutonium is used. For the total burn-up a reduction of the uncertainty from about 15 % to 12 % could be achieved.

3. The Breeding Ratio

3.1 Contributing reactions

The breeding ratio is defined as the ratio

$$\frac{\text{production of main fissile materials } (^{239}Pu,\ ^{241}Pu)}{\text{consumption of main fissile materials}}$$

Its value varies somewhat as burn-up proceeds; critical experiments aim mostly at the prediction of the initial breeding ratio, that is, at the beginning of life condition.

While the production of fissile materials occurs in comparable amounts in core and blanket (internal and external breeding), the consumption takes place almost completely in the core - there is a negligible correction for consumption in the blanket.

A rough estimate of the reactions occuring per fission neutron produced in the SNR-300 shows the relative contributions of the various reactions entering the breeding ratio for this reactor.

reactions in the core region	fission	^{239}Pu	0.26	C
	capture	^{239}Pu	0.07	C
	fission	^{240}Pu	0.015	
	capture	^{240}Pu	0.015	P
	fission	^{241}Pu	0.035	C
	capture	^{241}Pu	0.005	C
	fission	^{238}U	0.03	
	capture	^{238}U	0.15	P
	structural capture control rods, diluents		0.19	
reactions in the blanket region	capture	^{238}U	0.18	P
	leakage		0.01	
	others		0.04	
			1.00	

The reactions denoted with C and P are reactions consuming and producing main fissionable materials, respectively.
The breeding ratios derived from these numbers are:

Internal	0.45
External	0.49
Total	0.94

The main contributions clearly arise for consumption from ^{239}Pu fission and capture, for production from ^{238}U capture in core and blanket. Critical experiments therefore should concentrate on testing the accuracy of prediction for the ratio of these reaction rates.

3.2 Measurements in SNEAK-9 assemblies

The following measurements were performed with the aim of testing breeding ratio predictions:

- the ratio $^{238}U_{capt}/^{239}Pu_{fiss}$ at the center of SNEAK-9B and SNEAK-9C-2
- axial traverses of the same reaction rates through core and blanket of these assemblies
- radial traverses through the core of SNEAK-9C-2

The experimental technique used was foil activation. The average reaction rates inside the fuel and fertile material were derived either by placing the foils inside specially prepared perforated plates or by applying calculated corrections. For absolute calibration parallel plate fission chambers were used for ^{239}Pu fission and the Seufert-Stegemann method /19/ for ^{238}U capture.

3.3 Calculational methods

Calculations were performed for the central reaction rate ratios with the collision probability cell code KAPER /7/, for the axial traverses in one dimensional diffusion theory with cross sections also derived with the cell code KAPER. For the regions near the core-blanket boundary and for the transition into the deeper blanket a new cell code GITAN /20/ was developed by Böhme which allows a collision probability treatment of finite regions near zone boundaries. The radial flux variation was taken into account by group and material dependent bucklings (for diffusion calculations) or radius and zone-dependent source densities (in the GITAN calculations), both taken from two-dimensional diffusion calculations in RZ geometry. The radial traverses were directly compared to RZ diffusion calculations.

3.4 Results and discussion

The central reaction rate measurements show a clear overestimation of the reaction rate ratio $\frac{^{238}U \text{ capt}}{^{239}Pu \text{ fiss}}$:

$$C/E\left(\frac{^{238}U \text{ capt}}{^{239}Pu \text{ fiss}}\right) = 1.06 \text{ for SNEAK-9B}$$

$$= 1.069 \text{ for SNEAK-9C-2}$$

This overestimate is slightly larger than was found for previous assemblies (SNEAK-7A 1.042, 7B 1.051).

The traverses through the core for ^{239}Pu fiss are calculated slightly flatter with respect to the measurement than those for ^{238} U capt (Fig. 4). Thus the C/E value for ^{238}U capt/^{239}Pu fiss near the core boundary is reduced to 1.035 for SNEAK-9B and about 1.0 for 9C-2. This variation is brought about by the influence of spectral transients from the blanket. 1D Diffusion and GITAN transport calculation yield very similar results in this respect, they agree within 1 %.

In the outer parts of the SNEAK-9B axial blanket the measured values for ^{238}U capt become increasingly higher than the calculations, leading to an integral underestimate of ^{238}U capt of about 5 % in the blanket when measured and calculated traverses are normalized at the core boundary.

For the SNR-300 the following, still tentative conclusions may be drawn:

In the core, the volume integrated ratio of ^{238}U capt/^{239}Pu fiss should be overestimated by a factor of 1.05 with an uncertainty of about 0.02. Assuming agreement between measured and calculated spatial dependence of ^{238}U capt such a factor would also apply to the blanket. However,

the underestimate of the reaction rate in the outer blanket region causes a compensation, so that the C/E ratio for ^{238}U capt bl./^{239}Pu fiss core becomes close to unity. An uncertainty of 6 % must still be attached to this value. Of the remaining reactions entering the internal and external breeding ratio ^{239}Pu capt gives the largest contribution. This parameter was not measured in the SNEAK-9 cores, as no chance was seen to improve the present state of accuracy. However, it still causes the largest contribution (about 5 %) to the inaccuracy in the prediction of the breeding ratio.
In summary, the results are as follows

Contribution	C/E in SNEAK-9 (error is 1.7 σ)	Resulting deviation for SNR 300 breeding ratio (C - E)	Contribution to uncertainty of breeding ratio (∿ 1.7 σ)
$\frac{^{238}U \text{ capt. core}}{^{239}Pu \text{ fiss. core}}$	1.05 ± 0.02	0.02	0.01
$\frac{^{238}U \text{ capt. blank.}}{^{239}Pu \text{ fiss. core}}$	1.0 ± 0.06	--	0.03
$\frac{^{239}Pu \text{ capt.}}{^{239}Pu \text{ fiss.}}$	--	--	0.05
Total		0.02	0.06

If the capture traverse through the blanket is calculated by diffusion theory the underestimate there is increased and the resulting deviation for the SNR-300 breeding ratio becomes close to 0.

Finally one has to take in account that the criticality of a SNR-300 type reactor with present data and methods is overestimated by about 0.7 % (presumably by a combination of leakage underestimate, ^{238}U capt. overestimate and other, unidentified components). If this is compensated by increasing enrichment the total breeding ratio is lowered by about 0.01. If the compensation is brought about by adding fuel elements or withdrawing absorbers, no significant effect on the breeding ratio will result.

4. The Sodium Void Effect

4.1 Purpose of the experiments

It was the purpose of the sodium void measurements in the assemblies of the SNEAK-9 series to test and improve the reliability of prediction for specific cases in the SNR-300. The aim was pursued by measuring the effect in assemblies with compositions and spectra related to the SNR for a wide variation of parameters such as

void size, location and geometry
cell heterogeneity
plutonium isotopic vector

Since the cases of most interest for the SNR-300 are the maximum positive void effect and the effect of voiding single subassemblies the experiments concentrated on large voids with variing radius over one half or 2/3 of the core height and on axial voids of variing height in the central 4 SNEAK elements. (Corresponds about to one SNR-300 subassembly.)

As the magnitude of the sodium void effect depends decisively on the fuel used the experiments were performed only in the Pu-fueled assemblies SNEAK-9B and 9C. Composition and dimensions of the central zones of the SNR-300 were best approximated in SNEAK-9B (although the radius was still considerably too small), SNEAK-9C had a somewhat harder spectrum, and, due to the small core size, a particularly high leakage component. The degree of consistency in the difference between measurements and calculations for these two assemblies serves as a test for the possibility to extrapolate the results to the SNR-300.

4.2 Experiments performed

SNEAK-9B: (Core height 89.7 cm)

A central void of 60.84 cm height with the radial expansion increasing from 4 elements to 112 elements (corresponding to radii of 6.14 and 32.48 cm respectively).

Axial voids of increasing height centered on the core midplane in the four central SNEAK elements.

The same type of axial voids with a slightly modified cell which allowed to arrange the SNEAK platelets horizontally (as usual) or vertically in the element tubes. The measurements were made for both orientations.

SNEAK-9C-2: (Core height 60.5 cm)

A central void of 30.2 cm height radially increasing from 4 elements to 50 elements (corresponding to radii of 6.14 and 21.6 cm respectively).

A central void of 10.04 cm height and 6.14 cm radius in the basic assembly and in a test zone (POS) where the normal PuO_2UO_2 plates have been exchanged against the same type of plates with 19 % ^{240}Pu.

Axial voids of increasing height in 4 elements in the test zone POZ which used ZEBRA Pu-metal plates with 19 % ^{240}Pu in the 50 central core elements.

Axial voids of increasing heights in 4 elements in the test zone C where a carbide composition was simulated using the ZEBRA Pu-metal plates together with graphite in the central 50 core elements.

4.3 Methods of calculation

All experiments were calculated in two-dimensional perturbation theory in RZ geometry. For the axial traverses in SNEAK-9B first order perturbation was used, for all other cases exact perturbation (perturbed flux, unperturbed adjoint). Some cases involving compositions with increased ^{240}Pu contents were calculated using the k_{eff} difference method. Cell averaged cross sections were derived using the code KAPER /7/ except for the axial traverse in basic 9B where the older program ZERA /21/ was still used to facilitate comparisons with previous experiments. Direction dependent diffusion coefficients were used in the evaluation of the experiments with different plate orientations in 9B and in some of the high ^{240}Pu cases. A detailed study of the effect of cross section data, heterogeneity corrections and different calculational methods was performed for the case of radially increasing voids in SNEAK-9B /22/. It showed for exact perturbation theory and direct k_{eff}-calculations practically identical results while the values for first order perturbation lie about 20 - 30 % lower, with the largest deviations in the cases of the large voids. However for small voids in the high ^{240}Pu-zone POZ a comparison between exact perturbation theory and k_{eff} differences yielded discrepancies in the order of 10^{-5} in Δk amounting to 19 - 20 % of the measured effect.

For some cases the effect of increasing the ^{240}Pu capture cross section by 30 % was estimated using Δk_{eff} calculations with homogeneous cross sections.

4.4 Measured and calculated results

The most important results are given in Table 7 for large central voids, in Table 8 for small central voids and in Table 9 for axial voids of increasing height. The void radius for the maximum positive effect was barely reached for the large voids in SNEAK-9B but was reached and sur-

passed for the smaller core 9C-2.The axial voids always reached a maximum effect between one half and two thirds of the core height and decreased for larger void sizes.In general the comparison of measurements and calculations gave satisfactory results.When high ^{240}Pu SNEAK PuO_2UO_2 plates where introduced (9C-2/POS) a notable increase of the void effect was measured which was not reproduced ba calculations. Considerable discrepancies were found for the test zones POZ and C of SNEAK-9C-2,where the Pu-metal plates with high ^{240}Pu content from ZEBRA were used.In most cases a certain improvement could be reached by using Δk_{eff} difference instead of exact perturbation calculations, by introducing directional diffusion coefficients,and by introducing a correction for a 30% increased ^{240}Pu capture cross section. However the results of the k_{eff} difference calculations must be taken with caution since the effect is only about one order of magnitude larger than the convergence attainable.

4.5 Conclusions for the Na-Void Effect of the SNR

The preceding section shows that the reactivity effect of voids of the order of one subassembly or smaller can be predicted with an accurancy of about 2 ¢ (5 ¢ for carbide fuel).The direct measurement of larger voids yieled a maximum discrepancy of 6.5 ¢.However,such direct measurements were only performed with normal SNEAK fuel of only 8% ^{240}Pu contents.Therefore,in order to include the correct isotopic composition of the SNR 300 into the considerations one may extrapolate the discrepancies found in the high ^{240}Pu zones of SNEAK-9C to zones covering the whole core.Since the actual voids covered 4 of 138 elements the errors quoted above would extrapolate to the order of 60 ¢ (150 ¢ for carbide) for the whole core.

The fractional errors shown in the tables cannot be directly attributed to the SNR-300 since they are strongly dependent on the degree of compensation between the different components of the void effect. Since this compensation in the maximum void cases of the SNR 300 is considerably less pronouced than in SNEAK-9C the fractional error will become correspondingly smaller.So,at a maximum void effect of 3 $ for the SNR-300 a deviation

of 60 ¢ would amount to a fractional error of 20%.A conservative estimate thus would put the uncertainty of this effect for an oxide core at about 25% (1.7 σ).

Further experimental and analytical work is necessary to clarify the larger errors found to the carbide composition.Preliminary calculations with recently developed group constants indicate that a finer subdivision of energy groups may bring improvements.

Table 7 Measurements of Large Central Voids

Assby.	Core Height	Core Dia. (cm)	Void Height (cm)	Max.Effect Measured at Void Dia.	¢	C/E	C/E (¢)	Max.Void Dia. Reached (cm)
9B	89.7	108.3	60.8	65.0	79	1.08	6.5	65.0
9C-2	60.5	72.4	30.2	30.06	10.94	0.74	-2.9	43.4

Table 8 Measurements of Small Central Voids in 4 Elements

Assembly	Testzone	Void Height	Void Effect ¢	C/E	C-E (¢)
9B		10.15	1.7	0.92	-0.14
9C-2		10.01	1.84	1.0	0
9C-2	POS	10.04	2.84	0.69	-0.88
				0.97 a)	-0.08
9C-2	POZ	5.66	2.52	0.41 a)	-1.50
				0.43 a) b)	-1.45
9C-2	C	5.36	2.71	0.36 a)	-1.74
				0.37 a) b)	-1.70

a) k_{eff} difference calculation

b) includes preliminary correstion for 30% increased ^{240}Pu capture,calculated with homogeneous cross sections

Table 9 Measurements of Axial Voids in 4 Elements

Assembly	Core Height	Special Effect Investigated	Maximum Measured Effect at Void Height	ℓ	C/E	C-E(ℓ)	Effect of Void over Full Height ℓ	C-E(ℓ)
9B	89.7		60.9	6.1	0.9	-0.6	3.9	-1.5
9B		comparison of horizontal plate orientation [a]	60	5.6	1.0	0	3.1	-0.4
		and vertical plate orientation [a]	51	4.9	1.08	0.4	1.2	0.1
9C-2	60.04		30.2 [b]	3.34	1.0	0		
9C-2/POZ	60.2		39.6	3.45	0.54	-1.59	-0.80	
					0.69 [a)c)]	-1.07		-2.1 [a)c)]
					0.75 [a)c)d)]	-0.86		-1.98 [a)c)d)]
9C-2/C	58.56		37.5	5.97	0.31	-4.12	1.56	-2.95
					0.47 [a)c)]	-3.16		-5.60 [a)c)]
					0.51 [a)c)d)]	-2.93		-5.36 [a)c)d)]

a) Calculated with direction dependent diffusion coefficient

b) Largest axial void measured for basic 9C-2

c) Δk difference calculations

d) Includes a preliminary correction for 30 % increased ^{240}Pu capt., calculated with homogeneous cross sections

A trend is noticed that the agreement between calculations and measurements is improving as more refined calculational procedures and the latest cross section data are used in the interpretation.

5. Control Rod Worths

5.1 Scope of the experiments

During the SNEAK-9 critical experiments a number of different aspects of the problem of control rod worths were considered. These are:

- the reactivity worth of absorber samples in a composition similar to the SNR-300
- the effect of sodium voiding on the reactivity worths of absorber materials
- the reactivity worth and mutual interaction of rod banks in geometries similar to the SNR-300
- the reactivity of single rods in the vincinity of rod banks of different insertion configurations
- the reactivity of sodium followers versus normal fuel elements
- the worth of boron or sodium filled dummy elements at different locations in the core.

The measurements of the reactivity worth of absorber samples were performed by placing absorber rodlets in an aluminium matrix which was 12.1 cm high and had a cross section covering four SNEAK elements (Fig. 5). The holes in the matrix were arranged in such a way that the matrix in its cross section resembled an SNR-300 control rod when all holes except those in the four outer corners were filled with absorber. This and various other configurations in the matrix were investigated for the absorbers B_4C, Ta and Eu_2O_3. For the SNR-300 only the measurements with B_4C are of direct interest since this material is used in the control rods. The absorber matrix was placed in the assemblies SNEAK-9B, 9C-2 and the carbide version of this core, 9C-2/C. In general it was placed in the core center, some measurements for an eccentrical

position were performed in SNEAK-9B. Also in SNEAK-9B the measurements with all absorber positions in the aluminium matrix occupied were repeated in a core environment voided of sodium in order to determine the effect of sodium loss on the reactivity worth of control rods.

The measurements involving rod banks in SNR-300 geometry as well as the measurements on single rod characteristics, sodium follower worth and dummy elements were performed in SNEAK-9A. In this core the geometry of the SNR-300 was simulated as closely as possible. In order to achieve this ^{235}U fuel was used instead of PuO_2UO_2 which was not available in sufficient quantity. Core height and radius were about 0.9 times the corresponding SNR-300 dimensions. The following experiments involving banks of control rods were performed: Starting from the core 9A-1 (all rods simulated withdrawn) the rod bank RT 1, consisting of the three inner regulating rods, was introduced stepwise to complete insertion. Also, starting from 9A-1 the two regulating banks RT1 and RT2 (RT2 = the six outer regulating rods) were inserted simultaneously first 40, then 45 cm. Most rod bank experiments used the core 9A-2 as a reference which was critical with the banks RT1 and RT2 40 cm inserted. Starting from this position each bank separately and both banks together were stepwise brought to full insertion. Some further experiments involved the three safety rods which are located in the inner core zone near RT1.

The single rod experiments consisted of measuring the characteristics of one RT1 rod and of two RT2 rods in the vincinity of the reference position for various critical insertion configuration of the two rod banks.

The effect of replacing fuel by follower material was investigated in SNEAK-9A-0 which is the version of 9A without simulated control rods. The experiments were performed in a 4-Element-Group in the core center and in three such groups located symmetrically in eccentrical positions. The most important measurements were those in the core center because for this position calculations in RZ transport theory were possible.

Three types of element loadings were investigated in this experiment

1) Enriched uranium replaced by natural uranium
2) Elements loaded with Na-plates throughout core and axial blanket
3) Same as 2) except that Na in upper blanket was replaced by B_4C absorber

The reactivity worth of dummy rods containing B_4C absorber or just sodium such as are planned to be used in the first cycles of the SNR-300 was determined by introducing a group of four SNEAK elements with B_4C or Na loading at various radii in SNEAK-9A-2 in addition to the simulated control rods. The reactivity was measured as a function of the location of the simulated dummy rods.

5.2 Experimental methods

The quasicritical and various subcritical methods were used to perform the reactivity measurements for the control rod configurations described in the preceding section.

The quasicritical method consists in restoring criticality after changing the loading of simulated control rods by moving calibrated SNEAK regulating rods. Its range is restricted by the excess reactivity allowed to be held in the SNEAK rods which is limited to 1 %. It can be increased by loading additional edge elements when the excess reactivity is used up. In any such case the SNEAK regulating rods have to be recalibrated. The quasicritical method was used for all absorber measurements in the aluminium matrix in SNEAK-9B and 9C, for the sodium follower measurements in SNEAK-9A-0, for the characteristics of a single rod and a rod pair in SNEAK-9A-2, and for the measurements on simulated SNR-300 dummy rods, also in SNEAK-9A-2.

Subcritical measurements were performed for the determination of the reactivity of rod banks. Up to 7 % subcriticality were reached in these experiments. The measurement techniques used were subcritical source multiplication and source jerk. The source multiplication method is based on the inverse proportionality between neutron flux and subcriticality (1 - k) in point reactor theory. A ^{252}Cf source was placed into the core center, the flux was measured by two BF_3-ionization chambers and two ^{3}He-counters at the outer blanket boundary. Considerable calculated corrections had to be applied for changes in the spatial flux distribution and in the effective source strength as the simulated control rods were inserted into the core.

The source jerk method derives the subcriticality by an inverse kinetics method from the prompt jump and the following gradual decay of the flux when a source is suddenly removed from the core. The removal was achieved either by actually moving a ^{252}Cf source out to the core with a pile oscillator or by switching off a (d,T) neutron generator with the target in the core center after several minutes of running at constant pulse frequency and source strength. Corrections had to be applied for background radiation in the source-out position for the case of the Cf-source in the pile oscillator and for the different contributions of higher spatial modes with and without a source present in the core.

5.3 Calculational methods

The absorber measurements in the core center in the aluminium matrix were calculated by two-dim. RZ-diffusion theory using the code DIXY /6/ and the KFKINR cross section set in 26 groups. The cylindrical rodlets were smeared out in concentrical rings. Transport corrections were found by radial S8 calculations, geometry corrections by comparing 1 dim. cylinder calculations of the ring model to two-dimensional calculations of a model in XY geometry using the same axial buckling. In the cases with a single rodlet this was placed in the calculational model in the exact core center and smeared out with steel of the matrix tubes.

The measurements with control rod banks, the measurements with a single rod and a rod pair, and those with simulated B_4C and Na dummy elements (all in SNEAK-9A-1 or 9A-2) were calculated using the KASY synthesis code /9/ in XY/Z geometry with the cross sections condensated to four energy groups. Some of the rod bank experiments were also calculated using the Monte Carlo code MOCA /23/. Almost all of the rod bank experiments were also calculated using the MOXTOT /24/ cross section set condensated to 6 groups.

The sodium follower experiments in SNEAK-9A-0 were all calculated by 2 dim. RZ diffusion calculations in 26 groups. All cases of the central experiment except that of element type 1 (fuel exchanged against ^{238}U) were also calculated by 2 dim. transport theory since the conditions in the follower rods could not be treated with sufficient accuracy by diffusion calculations. In addition, some first order and exact perturbation calculations were performed. For calculating the experiment with three excentric followers, the rods were smeared out in rings and the calculations performed in 2 dim. RZ diffusion theory. A cylindrization correction was found as usual by comparing a 1 dim. radial and a 2 dim. XY calculation. The transport correction was taken over from the RZ calculations for the central rod.

5.4 Measured and Calculated Results

The most important results of the absorber measurements are summarized in Tables 10 to 15.

With respect to the reactivity worth of B_4C absorbers these tables give the following overall picture:

Table 10 Absorber Worth Measurements in SNEAK-9B and 9C-2 in the Aluminium Matrix (height 11.4 cm, cross section 4 SNEAK elements)

Assembly	Absorber Type	Loading [a]	Position	Measured Worth (¢)	C/E
9B	B_4C	4s.	central	-11.1	0.98
	B_4C	4s.+4b.	central	-40.8	1.00
	B_4C	4s.+8b.	central	-67.3	0.98
	B_4C	8s.+8b.	central	-76.6	0.98
	B_4C	8s.+8b.	central,in Na-void	-62.8	0.97
	B_4C	8s.+8b.	eccentric	-55.7	0.97
	B_4C	8s.+8b.	eccentric,in Na-void (near void boundary)	-49.0	1.01
	Ta	4s.	central	- 9.8	1.09
	Ta	8s.+8b.	central	-63.8	1.12
	Ta	8s.+8b.	central, in Na-void	-52.8	1.08
	Eu_2O_3	4s.	central	- 2.0	0.95
	Eu_2O_3	8s.+8b.	central	-14.6	0.67
9C-2	B_4C	4s.+8b.	central	-159.7	0.92
	$B_4C_{enr.}$	20 pins [b]	central	-304.5	0.76
	Ta	4s.+8b.	central	-137.3	1.03
	Eu_2O_3	4s.+8b.	central	-183.2	0.75
9C-2/C	B_4C	1s.	central,in carbide zone	- 6.12	0.98
	B_4C	4s.+8b.	central,in carbide zone	-152.9	0.9
	$B_4C_{enr.}$	1 pin [b]	central,in carbide zone	- 19.5	0.74
	$B_4C_{enr.}$	20 pins [b]	central,in carbide zone	-289.5	0.72

a) s. = small rodlet 13 mm dia.
b. = big rodlet 22 mm dia.

b) square MASURCA $B_4C_{enr.}$ pins $12.7 \cdot 12.7 \cdot 101.2$ mm^3

Table 11 Measurements with Rod Banks in SNEAK-9A-1 and 9A-2

Assembly	Rod Configuration RT1/RT2/A	Measured ($) a) b) S.M.	S.J.	C/E (S.M.) a) KFKINR 4 Gr.	MOXTOT 6 Gr.
9A-1	15/ 0/ 0	-0.51		0.85	0.91
	40/ 0/ 0	-2.29		0.93	1.00
	50/ 0/ 0	-3.17		0.95	--
	75/ 0/ 0	-5.02		0.95	0.99
	90/ 0/ 0	-5.44		0.94	0.99
	45/45/ 0	-5.07		0.97	1.02
9A-2	45/40/ 0	-0.41	-0.41	0.91	--
	60/40/ 0	-1.61	-1.63	0.93	0.98
	80/40/ 0	-2.76	-2.81	0.91	0.97
	90/40/ 0	-3.02	-2.98	0.90	0.98
	40/45/ 0	-0.46	-0.44	0.92	--
	40/60/ 0	-1.82	-1.80	0.92	0.95
	40/80/ 0	-3.13	-3.04	0.91	0.95
	40/90/ 0	-3.42	-3.37	0.89	0.94
	45/45/ 0	-0.87	-0.87	0.92	--
	60/60/ 0	-3.42	-3.45	0.93	0.99
	80/80/ 0	-5.89	-5.9	0.92 C/E(MOCA) c)	0.98
	90/90/ 0	-6.40	-6.5	0.91 0.87±0.10	0.97
	40/40/90	-4.27	-4.15	0.90 0.84±0.06	0.96
	0/63/90	-4.57	-4.35	0.87	0.94
	68/ 0/90	-4.03	-3.9	0.90	0.95
	90/90/90	-10.73	-10.5	0.90 0.87±0.04	0.96

a) S.M. = Source Multiplication S.J. = Source Jerk

b) Errors: Source Multiplication ∿ 5 % for all cases
Source Jerk: Increasing from 3% for small reactivities to ∿ 10 % for large reactivities

c) C/E for MOCA calculations using KFKINR set and S.M. results

Table 12 Mutual Influence of Rod Banks

Insertion depth (cm) (Ref.pos.: RT1,2: 40 cm, A: 0 cm)	$\Delta k(RT1)$		$\Delta k(RT2)$		$\Delta k(RT1+RT2)$		$\frac{\Delta k(RT1+RT2)}{\Delta k(RT1)+\Delta k(RT2)}$	
	Meas.	Calc.	Meas.	Calc.	Meas.	Calc.	Meas.	Calc.
60	-0.0114	-0.0106	-0.0129	-0.0119	-0.0243	-0.0227	1.0	1.01
80	-0.0196	-0.0179	-0.0222	-0.0203	-0.0418	-0.0385	1.0	1.008
90	-0.0214	-0.0193	-0.0243	-0.0217	-0.0454	-0.0413	0.993	1.007
	$\Delta k(RT_1+RT_2)$		$\Delta k(A)$		$\Delta k(RT1+RT2+A)$		$\frac{\Delta k(RT1+RT2+A)}{\Delta k(RT1+RT2)+\Delta k(A)}$	
90	-0.0454	-0.413	-0.0302	-0.0272	-0.0755	-0.0677	0.999	0.988

Table 13 Worth of a Single Rod and a Pair of Rods near the Reference Position

Reference position (RT_1/RT_2)	Rods moved	Av.Rod worth ($\frac{\not{e}}{cm}$)	C/E
40/40	1 RT1	-2.7	0.87
	1 RT2	-1.45	--
	2 RT2 (opposit)	-2.83	0.90
28/50	1 RT1	-2.26	0.85
	1 RT2	-1.55	--
	2 RT2 (opposit)	-2.97	--
58/20	1 RT1	-2.60	--
	1 RT2	-0.98	--

Table 14 Results of the Na-follower Experiment in SNEAK-9A-0

Control Rod Positions	Control Rod Loading	Δk Exp. against Ref.	C/E (RZ Diff.)	C/E (RZ-S6-Transp.)
1 central	type 1 fuel removed	-0.00797	1.048	
	type 2 sodium follower	-0.00596	1.096	1.003
	type 3 as type 2 B_4C in upper Bl.	-0.00660	1.079	0.999
3 eccentric	type 1	-0.02028	1.02	
	type 2	-0.01534	1.165	1.076

Table 15 Results of the Experiments with B_4C and Na Dummy Elements

Dummy Type	Dummy Position	Measured Worth $	C/E
B_4C	center	-2.44	0.86
	eccentric inner zone [a]	-1.73	0.86
Na	center	-0.57	1.03
	eccentric inner zone [a]	-0.45	1.02

a) Probable location for dummies in SNR-300

Experiment	C/E range	
B_4C in the Al-matrix in SNEAK-9B	0.97 - 1.01	
B_4C in the Al-matrix in SNEAK-9C-2 and 9C-2/C	0.90 - 0.98	
B_4C rod bank RT1 in 9A-1	0.93 - 0.97	except case 15/0/0
B_4C rod banks in SNEAK-9A-2	0.87 - 0.93	
Single B_4C rods and B_4C dummy element in the presence of 9 partially inserted rods in SNEAK-9A-2	0.85 - 0.90	
Enriched B_4C pins in the Al-matrix in SNEAK-9C-2 and 9C-2/C	0.72 - 0.76	

This survey shows that for measurements of the same group the results always are consistent within about 5 %, but that, as experimental conditions change the C/E ratio varies by a considerably larger amount. There is a clear tendency that the C/E value gets lower as the core becomes more densely loaded with B_4C. For natural boron it becomes lowest for the case when the insertion of single rods is changed in the presence of many partially inserted rods. Also, there is some indication that a hardening of the spectrum leads to lower C/E values.

In the voided environment the absorber worths are reduced due to the hardening of the spectrum. For both boron and tantalum the effect was well predicted by calculations. An exception is the case of an absorber near the void boundary where the reduction of the absorber worth is underpredicted leading to a 4 % increase in the C/E ratio.

The very low calculational values for enriched B_4C could not yet be explained. In order to do so further experiments on SNEAK and calculations of experiments with enriched B_4C on other facilities are being performed.

Table 12 shows results for the interaction of rod banks by comparing the sum of the reactivities of single bank insertions to the reactivity of combined insertion. Neither measurements nor calculations indicate a significant interaction which is typical for such a relatively small core.

The experiments in SNEAK-9A-0 (Table 14) and with Na-dummy elements in 9A-2 (Table 15) show clearly that the negativ worth of sodium filled elements versus normal fuel elements is always overestimated by diffusion theory. As for B_4C the C/E value becomes smaller when many partially inserted rods are present which is the case in the Na-dummy experiment in 9A-2. The S6-Transport calculations for the sodium follower experiment in 9A-0 show, that the overestimate can be eliminated by this method.

5.5 Significance for the SNR-300

The absorber measurements in the SNEAK-9 series covered a number of different aspects. It can be assumed that the following results are also valid for the SNR-300:

- The interaction between rod banks is quite small (of the order of 1 % in the reactivity range considered) according to measurements as well as calculations.
- The C/E ratio of the reactivity of follower and absorber rods in the presence of partially inserted rod banks is 5 - 10 % lower than in other measurements.
- Diffusion calculations overestimate the reactivity of followers vs. fuel elements by about 10 %. This error does not occur for S6-transport calculations.
- The effect of sodium void environment on control rod worths is well predicted.

The prediction of the absolute rod worths of the SNR-300 is affected by the poor prediction for B_4C(enriched) in the SNEAK experiments, since the SNR uses enriched boron in its control rods. The better prediction of enriched boron worth in ZPPR-4 by KfK methods and data /25/ seems to indicate that the misprediction for SNEAK-9C-2 is due to some specific error in this experiment or its interpretation. This problem has still to be solved before an absolute prediction of control rod worths in the SNR-300 can be derived from the measurements in SNEAK-9.

6. Power Distribution

6.1 Experiments performed

Measurements concerning the prediction of the power distribution were performed in assembly SNEAK-9A-2 which had the closest geometrical similarity to the SNR-300.

This assembly was built in three versions with the following amounts of insertion for the two regulating rod banks RT1 and RT2:

	Insertion in cm	
	RT1	RT2
normal core	40	40
1.modification	28	50
2.modification	58	20

Since the assembly was fueled with enriched uranium the distribution of ^{235}U fission and ^{238}U fission was measured.

The following measurements were performed:

Axial traverses by fission chambers in each version of the assembly in 31 core elements lying essentially on an East-West and a Southeast-Northwest trajectory through the core (Fig. 2).

Foil activations in the core midplane in the positions of the axial traverse measurements, further in several locations near the axial core-blanket interface.

Axial traverses by measuring the activation of SNEAK fuel plates in two elements of the inner zone and one element of the outer zone in each version of the assembly.

Horizontal scans by scanning the local activation across fuel plates in a number of adjoining SNEAK elements.

The axial fission chamber traverses are the main experiment on which the power mapping is based. The different traverses were interconnected through foil measurements at the core midplane and by calibrating the fission chambers in a reactor region were the absolute fission rate was measured.

The axial distribution measured with SNEAK plates and foils was mainly used as a check on the traverses measured with fission chambers. In general a good agreement was found, however, a close examination of the traverses shows that the chamber traverses were slightly too flat as compared to the activation traverses (Fig. 6). This is probably due to the perturbation of the core properties by the axial channel (streaming). A correction was derived for the fission chamber results which reaches 1.5 % for Z = $\pm$ 45 cm.

6.2 Method of calculation

Three-dimensional calculations were performed using the flux synthesis program KASY /9/ with KFKINR cross sections condensed to four energy groups (1-4, 5-6, 7-10, 11-26).

For the fuel regions heterogeneous cross sections calculated with the code ZERA /21/ were used. The perturbations introduced by SNEAK shim rods and by rest cells were not considered.

Trial functions for use in the synthesis calculations were calculated in XY geometry for the core with follower material in the RT positions, with absorber in one RT bank and follower in the other (only necessary for first and second modification), and with absorber in both RT banks. No blanket trial functions were used. The mesh spacing was 2.72 cm in the X- and Y-direction.

For some selected cases test calculations using more elaborate methods were performed. The effect of the following calculational refinements was studied: Halfing of the mesh space, introduction of a blanket trial function, and increasing the number of groups to 6 and 12. The effect was always of the order of 0.1 % near the core center and 1.0 % at locations of large gradients. The conclusions with respect to maximum to average fluxes as given below are not affected by these calculational modifications. A comparison of transport and diffusion calculations for a central rod in RZ-geometry shows that the shift of the axial flux peak which is observed between diffusion theory and experiment is significantly reduced when transport theory is applied.

6.3 Results

The main quantities of interest for a comparison between measurements and calculations are:

- the integral axial power of an element as a function of the horizontal position
- the axial form factor, that is, maximum to average power for a given element position

- the maximum to average power for the whole core, which can be derived from the above two quantities
- the exact position of the power maxima.

A map of the deviations between measurements and calculations for the integrated axial power is given in Fig. 7. It shows an underestimation in the core center, a corresponding overestimation at the outer edge of the inner and the outer core zone and varying deviations at the flux maximum on the inner edge of the outer core zone.
On the whole, this means, that the flux is calculated too flat, which, in most cases, is also true for the axial traverses.

Table 16 compares calculated and measured properties of the power distribution at positions of relative power maxima and at a position near a simulated control rod in the three versions of the core SNEAK-9A-2.

The parameters considered are the integrated axial power (normalized to unity for the average of all traverses measured), the axial form factor and the ratio of maximum power in an element to average core power.

Also the position of the axial power maxima and the error made in calculating this position is given.

Just as the integrated axial power also the local power maximum is calculated slightly too low at the core center, while no unique trend can be found at the inner edge of the outer zone. The flux maximum near a simulated partially inserted control rod is calculated too low, the flux shift caused by the rods is underestimated by the calculation which can be seen from Fig. 6 as well as from the last two lines of Table 16.

Results which because of the similarity in geometry and nuclear properties should be transferrable to the SNR-300 are the following:

Table 16 Results for Power Distribution in SNEAK-9A-2

Core		Normal Core				1. Modification				2. Modification			
Regulating Rod Insertion RT1/RT2		40/40				28/50				58/20			
Element Position		18-20	26-25	18-11	19-22	18-20	26-25	18-11	19-22	18-20	26-25	18-11	19-22
Significance of position		Core Center	Boundary	Power Maximum at Zone	Position near Regulating Rod	Core Center	Boundary	Power Maximum at Zone	Position near Regulating Rod	Core Center	Boundary	Power Maximum at Zone	Position near Regulating Rod
Integrated Axial Power	E	1.13	1.22	1.23	1.08								
	$\frac{C-E}{E}$	-0.014	0.009	-0.004	-0.015	-0.018	0.007	-0.004	-0.023	-0.009	0.005	-0.006	-0.004
Form factor	E	1.273	1.256	1.259	1.315	1.270	1.246		1.292	1.229	1.248		1.246
	$\frac{C-E}{E}$	0.007	-0.005	-0.008	-0.007	0.002	-0.002		-0.006	-0.011	0.002		-0.014
$\frac{\text{Max.Power}}{\text{Av. Power}}$ (total core)	E	1.51	1.61	1.63	1.49								
	$\frac{C-E}{E}$	-0.007	0.004	-0.012	-0.022	-0.016	0.005		-0.029	-0.020	0.007		-0.018
Ax. Position of (cm from midplane)	E	-7.5	-7.0	-6.0	-8.5	-6.0	-6.0		-6.5	-10.0	-4.5		-18.0
Maximum	C-E	0.0	1.5	1.0	0.0	2.5	1.0		1.5	- 3.0	1.0		2.5

In most parts of the core the power distribution is predicted correctly within 2 %. Somewhat larger deviations occur in regions with strong flux gradients.

The power distribution is predicted slightly too flat, resulting in an underestimate (< 1 %) of the power maximum in the core center.

Diffusion theory in general underestimates the flux shift caused by partially inserted control rods, resulting in an underestimate of the power in the upper core half, an overestimate in the lower core half and an upward shift of the calculated position of the power maximum.

7. Influence of the Delayed Neutron Fraction

In the evaluation of all reactivity measurements in SNEAK-9 delayed neutron fractions as originally quoted by Keepin /26/ have been used.

During the past years thorough reviews of the delayed neutron data have been performed, mainly motivated by the central worth discrepancy, that is, a rather regular overestimate of the central reactivity worth of the main fissile materials.

Also, experiments about delayed neutron data have been performed in SNEAK assemblies 7A, 7B, 9C-1 and 9C-2 /17/. β_{eff} was determined by measuring the apparent central reactivity worth of a ^{252}Cf-source and by an experimental determination of the normalization integral.

The ratio of β for various isotopes was found by studiing the effect of the transport of delayed neutron precursors for these isotopes. For this purpose a uniformly loaded pile oscillator was moved through the core; this had to be done for various isotopic compositions of the loading.

The results of the SNEAK measurements agree best with the evaluation of Tuttle /18/. This means, with respect to the Keepin data the delayed neutron yield per fission has to be increased by about 4 % for ^{235}U, 6 % for ^{239}Pu and 10 % for ^{238}U.

Further it was found that Keepin's delayed neutron fractions used in SNEAK evaluations were taken from measurements in very hard spectra. However, with changing spectra the delayed neutron fraction changes inversely proportional to ν as the delayed neutron yield per fission, $\nu\beta$, stays about constant. For this reason the presently used data are about another 2 % too low.

In summary, this means that β_{eff} has to be increased by about 8 % for Pu-cores and 6 % for ^{235}U-cores.

In Table 17 β_{eff}-values derived from Keepin (as used in all the evaluations) and derived from Tuttle are compared for the basic SNEAK-9 assemblies. The effect of using the Tuttle data in predicting the burn-up reactivity is discussed in section 2.6. The value of β_{eff} also effects the evaluation of the absorber worth and the sodium void measurements. With the Tuttle data the C/E ratios would be lowered by 6 - 8 %. For the absorber worths this means a somewhat increased discrepancy between measurements and calculation. For the Na-void effect there are cases where the agreement is improved and others where it gets worse. The degree of consistency of the results is not affected, since a change in β_{eff} enters the C/E-ratios for all reactivity measurements in a given assembly as a constant factor.

Table 17 Delayed Neutron Fractions (in 10^{-2}) for SNEAK-9 Assemblies

Assembly	9B	9A	9C-1	9C-2
Original Keepin Data	0.443	0.710	0.706	0.372
Tuttle Data	0.479	0.752	0.754	0.404

8. Conclusions

A review of the results compiled in this report leads to remaining uncertainties for the prediction of physics parameters of the SNR-300 as given in Table 18. It must be noted that the numbers in this table necessarily contain a certain amount of personal judgement. A comparison is made with the values of Table 1 of /27/ where the accuracies which will be reached after the critical experiments program were predicted. It shows that the projected accuracies could be reached or surpassed in most instances. For the measurements of the Na-void effect, the interpretation is still not satisfactory although the extrapolation of the discrepancies found to the SNR-300 do not lead to uncertainties far beyond the target accuracy. Also an unexpectedly large deviation was found between measurement and calculation of the reactivity worth of enriched B_4C.

The relatively large uncertainty in the prediction of the sodium void effect is mainly suggested by the results of the experiments involving the ZEBRA high ^{240}Pu metal plates. The other results of Na-void experiments indicate an accuracy of prediction of the maximum effect within the projected value of 20 %. The uncertainty in the prediction of the worth of enriched B_4C stems from measurements with MASURCA enriched B_4C rodlets in SNEAK-9C-2. The other absorber measurements were conducted using natural B_4C. This means, the large discrepancies only appear in a few specific experiments. An improvement of confidence in the prediction of the parameters concerned can be brought about by performing and evaluating new experiments or by evaluating comparable experiments which have been performed on other facilities. These routes are being followed in different activities.

For the other parameters investigated (k_{eff}, breeding ratio, power distribution) the results of the SNEAK-9 series show an accuracy and consistency in prediction which corresponds to our present experimental and theoretical possibilities.

Table 18 Uncertainty of SNR-300 Physics Parameters According to Best Judgement after Evaluation of SNEAK-9 Experiments (Confidence about 90 % ≙ 1.7σ)

Parameter	Uncertainty [%]	Uncertainty predicted in /27/
k_{eff}	0.7	1.3
breeding ratio	6	6
Ma. Na-void	25	20
absorber worth (natural B_4C)	7	8
absorber worth (enriched B_4C)	17	
power distribution (local/average)	4	4
power distribution (peak/average)	2	

References

/1/ G. Jourdan et al.
Physics Investigations of Sodium Cooled Fast Reactors;
SNEAK Assembly 9B
KFK 2012 (1974)

/2/ M. Pinter et al.
Physics Investigations of Sodium Cooled Fast Reactors;
SNEAK Assembly 9A
KFK 2028 (1974)

/3/ M. Pinter et al.
Control Rod Worth and Power Distribution Measurements in the SNR Mock Up SNEAK Assembly 9A
KFK 2077 (1974)

/4/ W. Scholtyssek et al.
Physics Investigations of Sodium Cooled Fast Reactors;
SNEAK Assembly 9C
KFK 2361 (1977)

/5/ E. Kiefhaber
The KFKINR-set of Group Constants; Nuclear Data Basis and First Results of its Application to the Recalculation of Fast ZERO-Power Reactors
KFK 1572 (1972)

/6/ W. Hoebel
"DIXY", Unpublished Computer Program,
Kernforschungszentrum Karlsruhe

/7/ P.E. McGrath
KAPER - Lattice Program for Heterogeneous Critical Facilities
KFK 1893 (1973)

/8/ REMO, unpublished computer program, Kernforschungszentrum Karlsruhe. Basic equations in: H. Huschke, Gruppenkonstanten für dampf- und natriumgekühlte schnelle Reaktoren in einer 26-Gruppendarstellung
KFK 770 (1968)

/9/ G. Buckel
Approximation der stationären dreidimensionalen Mehrgruppen-Neutronen-Diffusionsgleichung durch ein Syntheseverfahren mit dem Karlsruher Syntheseprogramm KASY
KFK 1349 (1971)

/10/ E.A. Fischer, P.E. McGrath
Physics Investigations of two Pu-Fueled Fast Critical Assemblies: SNEAK-7A and 7B
KFK 1939 (1974)

/11/ H. Giese et al.
Physics Investigations of a Compact Simulation of a Large Fast Breeder Reactor, SNEAK Assembly 10
KFK 2573 (1978)

/12/ J.P. Chaudat, M. Darrouzet, E.A. Fischer
Experiments in Pure Uranium Lattices with Unit k_∞. Assemblies SNEAK-8/8Z; UK 1 and UK 5 in ERMINE and HARMONIE
KFK 1865
CEA-R-4452 (1974)

/13/ F. Helm et al.
Physics Investigations of Sodium Cooled Fast Reactors; SNEAK Assembly 2
KFK 1399 (1971)

/14/ F. Helm
Auswertung der Sektorsubstitution SNEAK-9C-1/9C-2
KFK 1275/2 PSB 2. Vierteljahresbericht 1975, pg. 121-1

/15/ S. Pilate
Private communication (August 1974)

/16/ S. Pilate et al.
Use of ZPPR Measurements as a Support of Criticality Prediction for SNR-300
Trans. Am. Nucl. Soc. 24, 483 (Nov. 1976) (see also Ref. /25/)

/17/ E.A. Fischer
Integral Measurements of the Effective Delayed Neutron Fractions in the Fast Critical Assembly SNEAK
Nucl. Sci. Eng. 62, 105, (1977)

/18/ R.J. Tuttle
Delayed Neutron Data for Reactor Physics Analysis
Nucl. Sci. Eng. 56, 37, (1975)

/19/ H. Seufert and D. Stegemann
A Method for Absolute Determination of ^{238}U Capture Rates in Fast Zero Power Reactors
Nucl. Sci. Eng. 28, 277, (1967)

/20/ R. Böhme
Integrale Transporttheorie mit linearer Anisotropie der Streuung zur Berechnung der Neutronenverteilung in endlichen Plattenanordnungen Schneller Reaktoren
KFK 2501 (1977)

/21/ D. Wintzer
Zur Berechnung von Heterogenitätseffekten in periodischen Zellstrukturen thermischer und schneller Kernreaktoren
KFK 743 (1969)

/22/ G. Jourdan
Messung und Berechnung des maximalen Na-void Effektes in einem Plutonium-Reaktor vom SNR-Typ
Reaktortagung Karlsruhe (1973) Proc. pg. 83

/23/ J. Lieberoth
A Monte Carlo Technique to Solve the Static Eigenvalue Problem of the Boltzmann Transport Equations
Nucleonics 11, Vol. 5, 213 (1968)

/24/ E. Kiefhaber and J.J. Schmidt
Evaluation of Fast Critical Experiments Using Recent Methods and Data
KFK 969 (1970)

/25/ S. Pilate et al.
Use of ZPPR Measurements as a Support of Criticality Prediction for SNR-300
Nuclear Technology, to be published (see also Ref. /16/)

/26/ G.R. Keepin
Physics of Nuclear Kinetics
Addison-Wesley Publ. Comp., Inc., (1965)

/27/ D. Wintzer et al.
Unsicherheiten bei der Voraussage wichtiger neutronenphysikalischer Parameter des SNR-300 und großer Leistungsbrüter und Reduzierung dieser Unsicherheiten durch SNEAK-Experimente
Reaktortagung Karlsruhe (1973) Proc. pg. 147

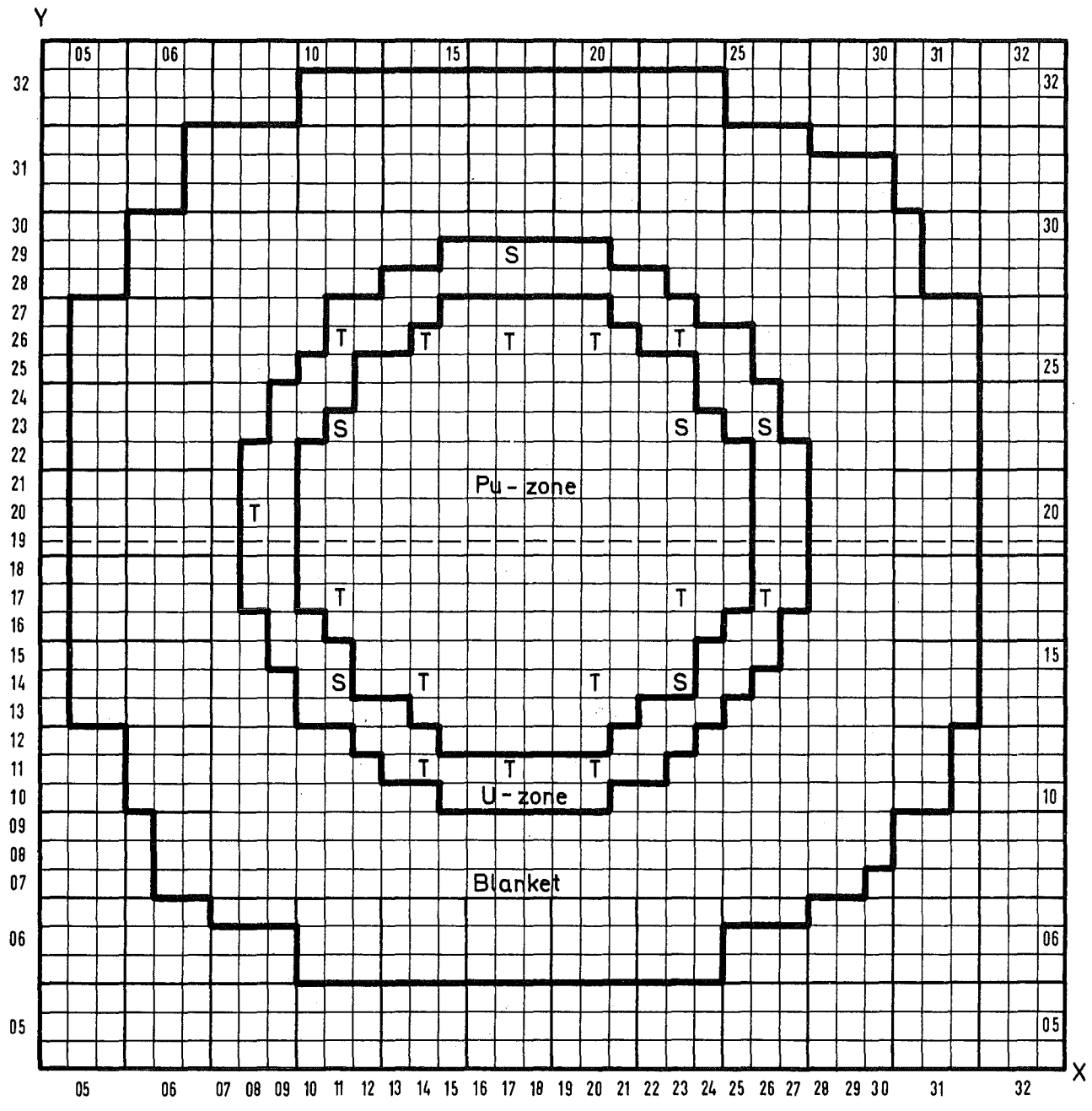

SNEAK - 9B Cross Section of the Critical Configuration

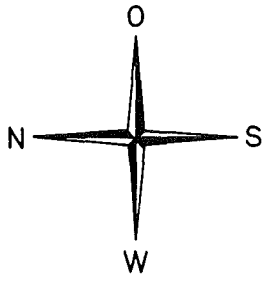

S = Safety rod

T = Shim rod

——— = Radial channel

Fig. 1

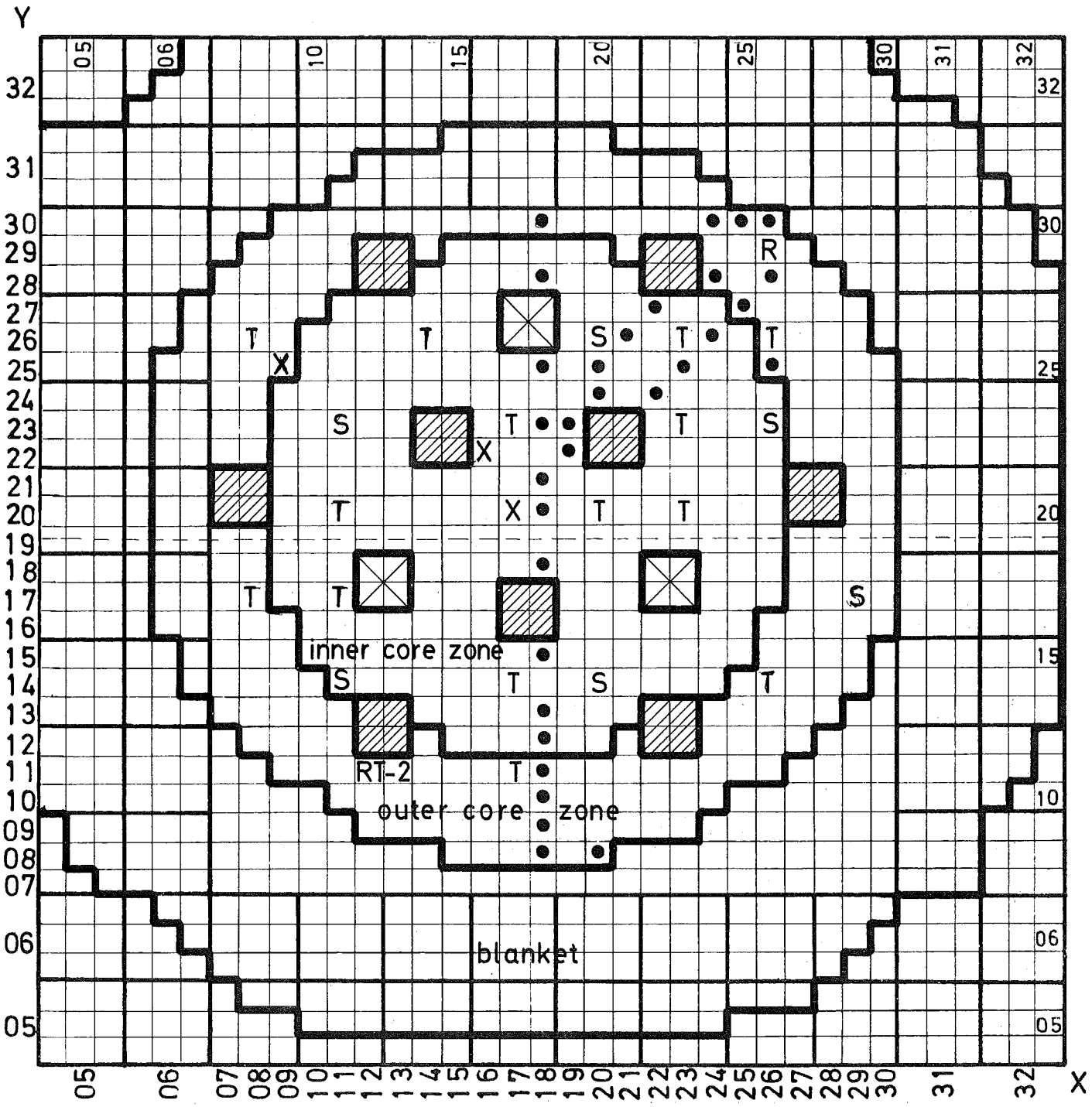

Fig. 2 SNEAK-9A-2

Simulated SNR control rod (RT-1, RT-2)

Simulated SNR safety rod

Position of axial traverse measured with
x SNEAK platelets ● fission chambers

S = SNEAK safety rod, T = SNEAK schim rod, R = SNEAK control rod

Maßstab 1:10

O
N
S
W

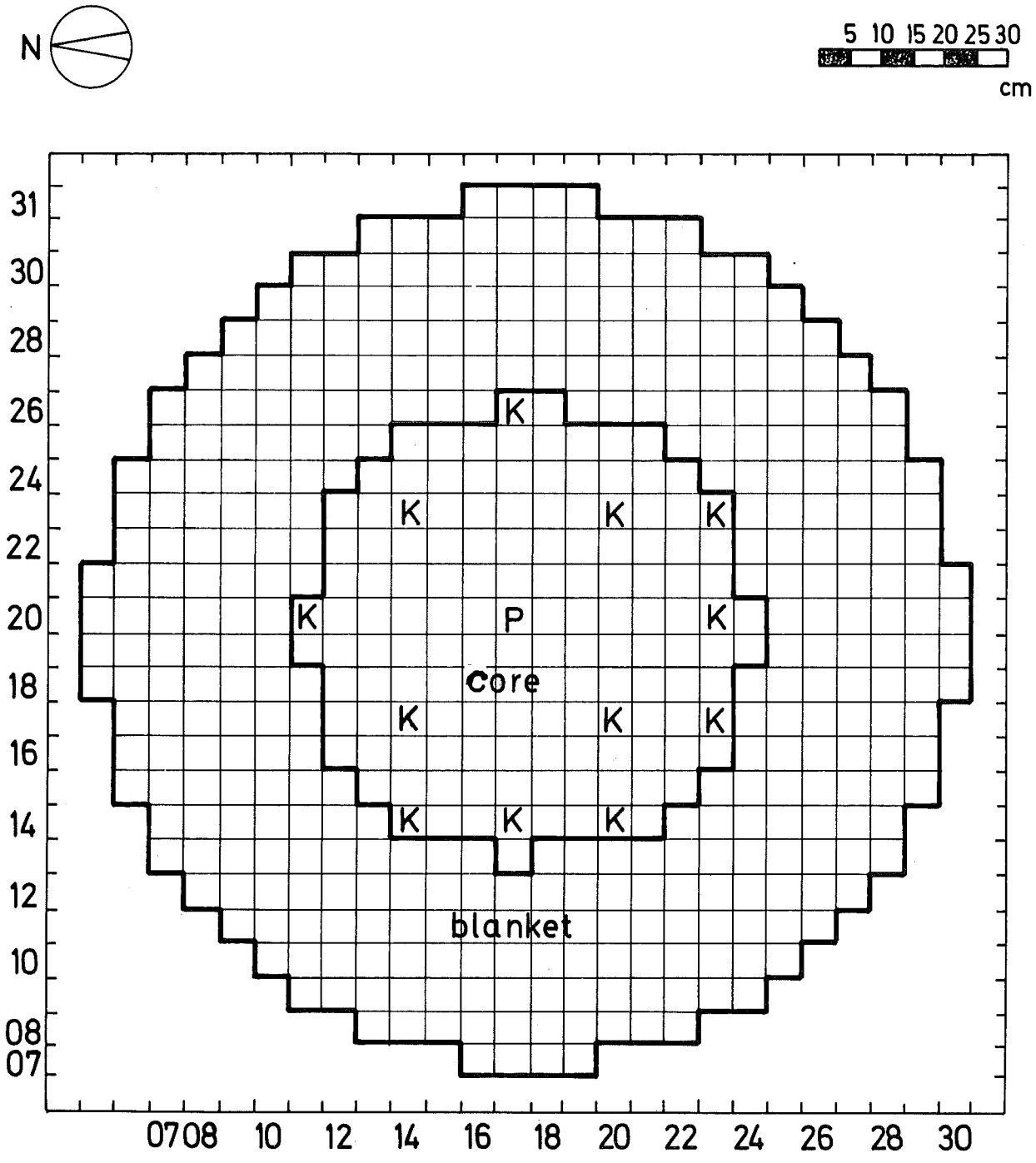

Fig. 3 Cross section of SNEAK 9C-2 critical experiment

K SNEAK control element

P Position for pile oszillator

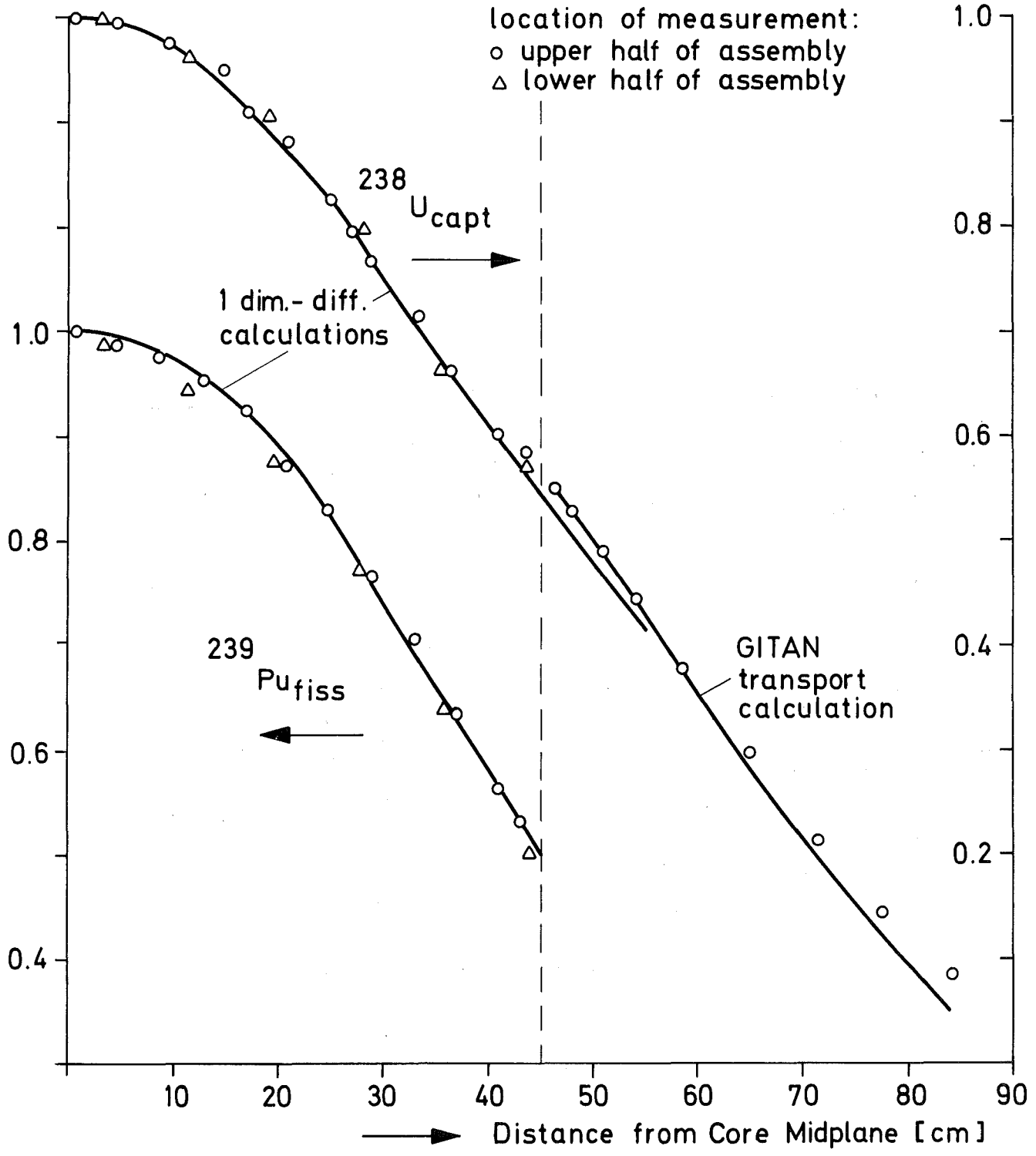

Fig. 4 Axial Reaction Rate Traverses in SNEAK 9B

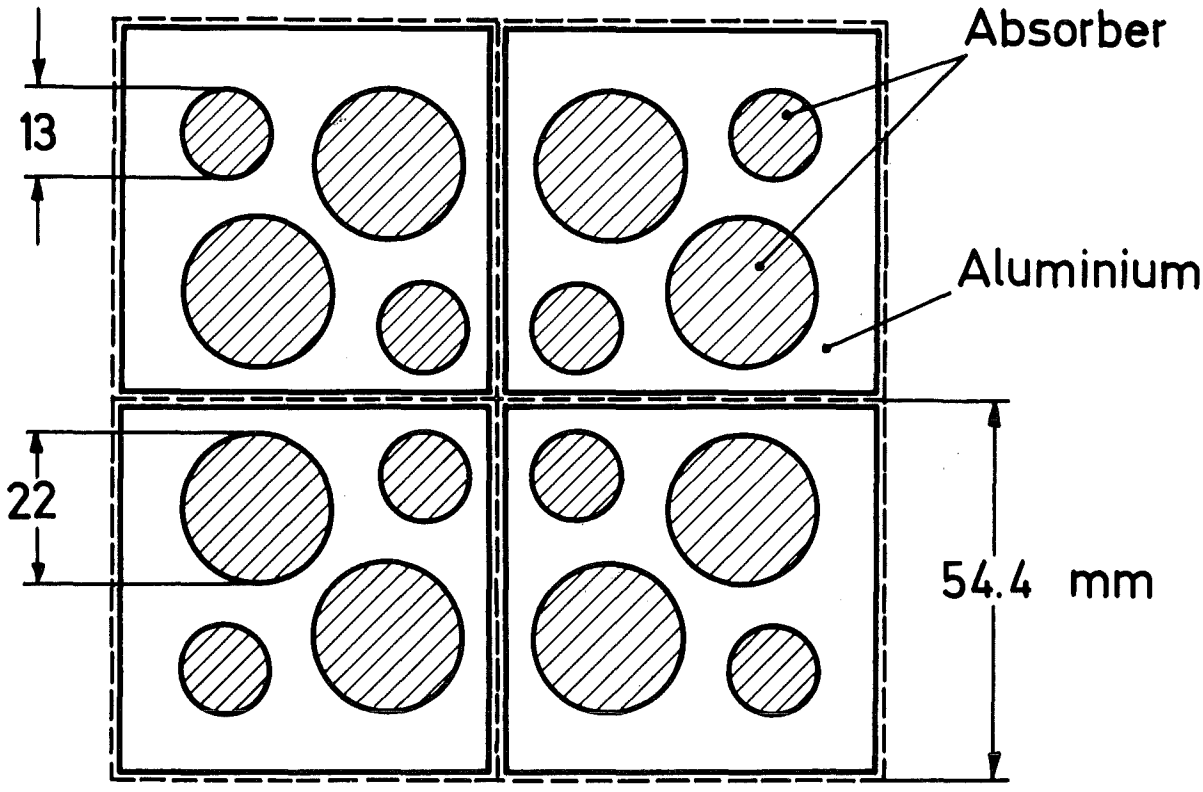

Fig. 5 Cross Section of Absorber Zone

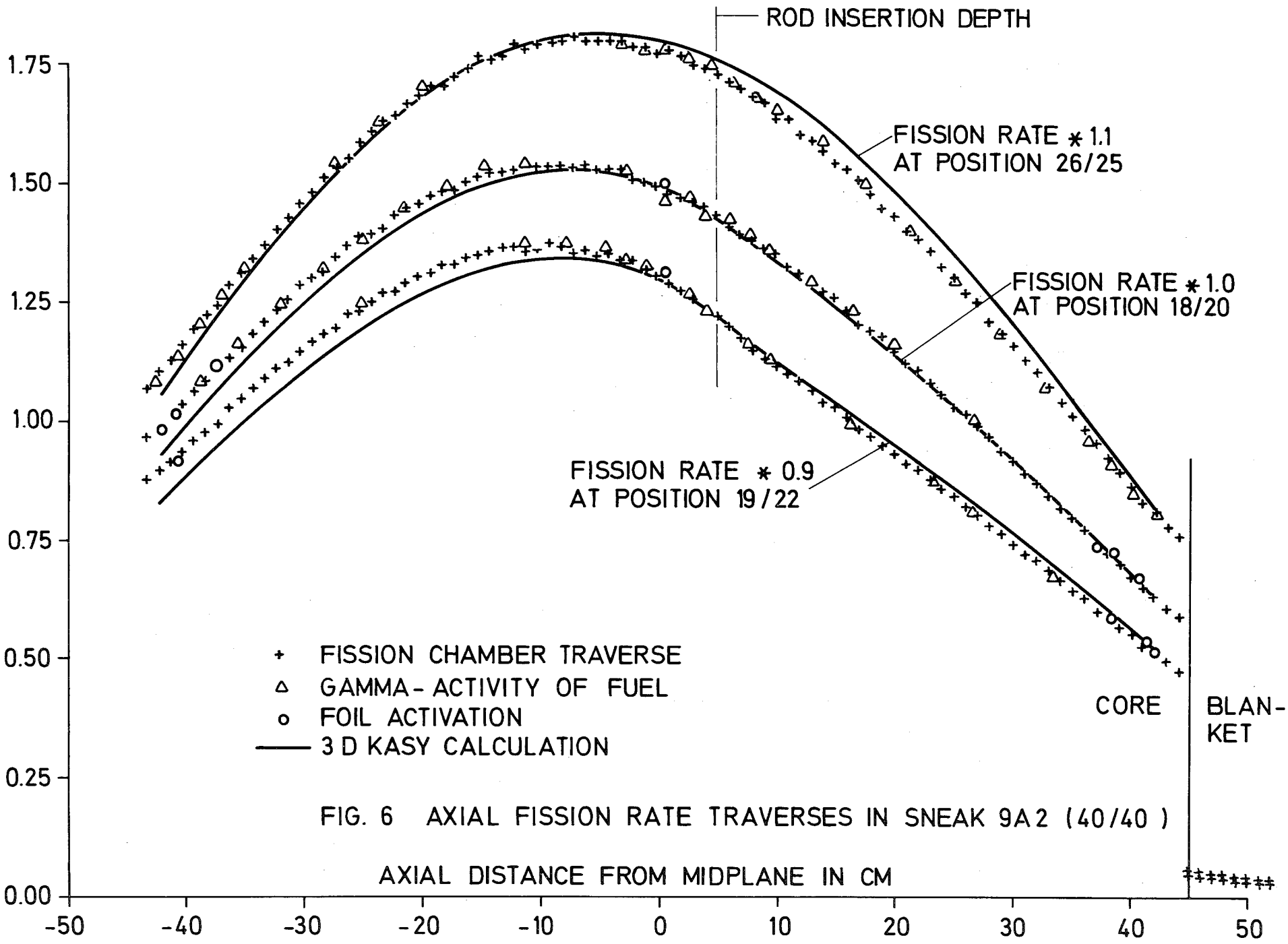

FIG. 6 AXIAL FISSION RATE TRAVERSES IN SNEAK 9A2 (40/40)

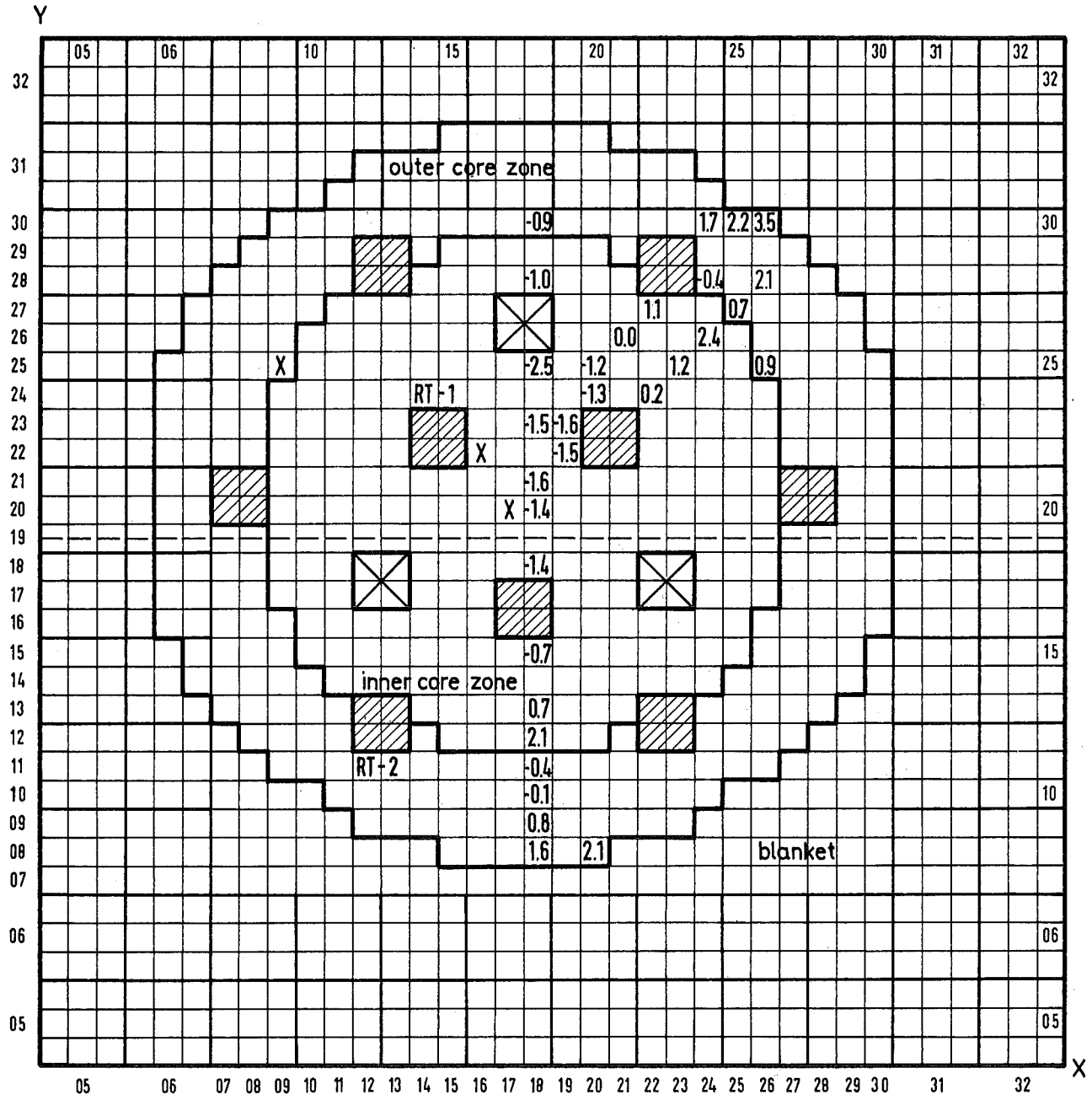

SNEAK-9A2 First Core (40/40)

Relative Deviations of Axial Integrals

$$\left(\frac{C-E}{E} \text{ in } \%\right)$$

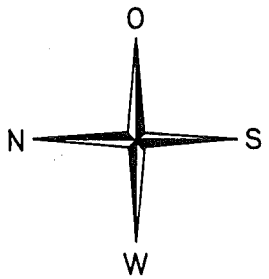

Fig. 7